Wavelet Orthonormal Decomposition for Extracting Features in Pattern Recognition

Yuan Y. Tang

Department of Computing Studies
Hong Kong Baptist University
Kowloon Tong, Hong Kong

Abstract

In this paper, a novel approach based on the wavelet orthonormal decomposition is presented to extract features in pattern recognition. The proposed approach first reduces the dimensionality of a two-dimensional pattern, and thereafter performs wavelet transform on the derived one-dimensional pattern to generate a set of wavelet transform sub-patterns, namely, several uncorrelated functions. Based on these functions, new features are readily computed to represent the original two-dimensional patterns. As an application, experiments were conducted using a set of printed characters with varying orientations. The results obtained from these experiments have consistently shown the proposed feature vector can yield an excellent classification rate in pattern recognition

1 Introduction

Wavelet analysis and its applications have become one of the fastest growing research areas in the recent years [2]. This is in part attributed to the pioneering work by the researchers as well as practitioners in the field of signal processing. Morlet first coined down the term of *wavelet analysis* in early 1980's. In 1986, Meyer developed a wavelet basis, which is best known today as Meyer's basis. Later, Mallat and Meyer formulated a theory of multiresolution analysis theory, and subsequently, proposed the Mallat algorithm, making wavelet transform readily implementable with digital computers. In 1990's, advanced research and development in wavelet analysis has found numerous applications in such areas as signal processing, image processing, and pattern recognition with many encouraging results [8]. During this fast growth in theories and applications, the theoretical development of high-dimensional wavelet analysis is somewhat lagging behind as compared to that of the one-dimensional wavelet. As has been shown in several real-life applications, the two-dimensional wavelet analysis has not been as effectively applied as the one-dimensional analysis.

Through mathematically sound derivations, the goal of this paper is to reduce the problem of two-dimensional patterns into that of one-dimensional ones, and thereafter, utilize the well-established one-dimensional wavelet transform coupled with other techniques to extract feature vectors from the one-dimensional patterns.

The present study explores the use of our previous work [7] in reducing the dimensionality of two-dimensional patterns into one-dimensional ones. Consequently, we can perform wavelet transform on the derived one-dimensional patterns to generate a set of *wavelet transform sub-patterns* which are a set of uncorrelated one-dimensional functions, i.e. non-self-intersecting curves. We then extract the features from the individual curves. This allows us to map the set of non-self-intersecting curves into a feature vector corresponding to the original two-dimensional patterns.

The overall sequence of presentation of this paper is illustrated below:

- Construction of one-dimensional orthonormal wavelet basis
- Wavelet orthonormal decomposition to produce sub-patterns
- Experiments
- Conclusions

2 Construction of 1-D Orthonormal Wavelet Basis

In pattern recognition, a one-dimensional pattern, $f(x)$, can always be viewed as a signal of finite energy; i.e.,

$$\int_{-\infty}^{+\infty} | f(x) |^2 \, dx < +\infty$$

This is also mathematically equivalent to say, $f(x) \in L^2(I\!R)$. Here, we shall apply multiresolution analysis [6] in order to obtain the orthonormal wavelet basis of $L^2(I\!R)$ space, and furthermore, decompose one-dimensional patterns pertaining to$L^2(I\!R)$ space, with the obtained orthonormal wavelet basis.

In the beginning of this section, we shall describe the formulation of one-dimensional orthonormal wavelet basis of $L^2(I\!R)$ space, utilizing multiresolution analysis [4, 5].

Definition 2.1 Let us consider a sequence of closed sub-spaces $\{V_j\}_{j \in Z\!\!Z}$ of $L^2(I\!R)$. This sequence is called a multiresolution analysis (MRA) if the sub-spaces have the following properties:

1. $V_j \subset V_{j-1}$ for any $j \in Z\!\!Z$;
2. $\cap_{j \in Z\!\!Z} V_j = \{0\}$ and $clos_{L^2}(\cup_{j \in Z\!\!Z} V_j) = L^2(I\!R)$;
3. $u(x) \in V_j \Longleftrightarrow u(2x) \in V_{j-1}$;
4. $u(x) \in V_0 \Longrightarrow u(x-k) \in V_0$ for any $k \in Z\!\!Z$; and
5. There exists a function $g(x) \in V_0$, such that $\{g(x-k) | k \in Z\!\!Z\}$ constitutes a Riesz basis of V_0. That means let l^2 denote the space of all square-summable bi-infinite sequences; that is, $\{a_k\} \in l^2$ if and only if

$$\sum_{n=-\infty}^{\infty} |a_k|^2 < \infty.$$

For any $u \in V_0$, there exists a unique $\{a_k\} \in l^2$, we have

$$u(x) = \sum_{k \in Z\!\!Z} a_k g(x-k).$$

In the above-listed properties, $Z\!\!Z$ denotes all the possible integers, and function $g(x)$ is called *generating function.* It should be noted that based on Property 4, the following can be deduced; namely: $u(x) \in V_0$ *is equivalent to* $u(x-k) \in V_0$. Moreover, Properties 1 and 3 imply that as a closed subspace of $L^2(I\!R)$, V_{j-1} is greater than V_j. The difference between V_{j-1} and V_j corresponds to exactly the high-frequency signal component of V_{j-1}. From functional analysis, it is known that V_{j-1} can be decomposed orthogonally, as follows:

$$V_{j-1} = W_j \oplus V_j \tag{1}$$

where W_j contains the high-frequency signal component of V_{j-1}, and V_j contains the low-frequency signal component of V_{j-1}.

In other words, Eq. (1) indicates that signals in V_j are the simple linear summation of the high-frequency signals in W_j and the low-frequency signals in V_{j-1}. Besides, Property 4 of Definition 2.1 also tells us that the basis of V_0 is composed of $\{g(x-k), k \in Z\!\!Z\}$, which are not necessarily orthonormal. In order to obtain orthonormal wavelet basis, we need to introduce the notion of a *scaling function.* The scaling function $\varphi(x)$ is deduced from the generating function $g(x)$ as follows:

Definition 2.2 The scaling function $\varphi(x)$ is defined as follows

$$\varphi(x) = \frac{1}{\sqrt{2\pi}} \left[\frac{\hat{g}(w)}{\sqrt{\sum_{k \in Z\!\!Z} |\hat{g}(\omega + 2k\pi)|^2}} \right]^{\vee}, \tag{2}$$

$$\hat{g}(w) = \frac{1}{\sqrt{2\pi}} \int_R g(x) e^{-j\omega x} dx,$$

where, $\hat{g}(w)$ denotes the Fourier transform of $g(x)$, the superscript $[*]^{\vee}$ stands for the inverse Fourier transform of $[*]$.

Theorem 2.1 The translation of scaling functions $\{\varphi(x-k) | k \in Z\!\!Z\}$ is an orthonormal base for V_0, and $\varphi_{j,k}(x) = \{2^{-j/2}\varphi(2^{-j/2}x - k) | k \in Z\!\!Z\}$ is an orthonormal base for V_j.

In order to prove this theorem, the following lemma needs to be proved first:

Lemma 2.1 The necessary and sufficient condition to constitute an orthonormal set by $\{\varphi(x-k) | k \in Z\!\!Z\}$ is as follows:

$$\sum_{k \in Z\!\!Z} |\hat{\varphi}(\omega + 2k\pi)|^2 = \frac{1}{\sqrt{2\pi}}. \tag{3}$$

Specifically, we consider a significant equation referred to as two-scale equation.

$$\frac{1}{\sqrt{2}} \varphi(\frac{x}{2}) \in V_1 \subset V_0,$$

we have

$$\frac{1}{\sqrt{2}}\varphi(\frac{x}{2}) = \sum_{k\in\mathbb{Z}} h_k\varphi(x-k), \tag{4}$$

where

$$\begin{aligned} h_k &= <\frac{1}{\sqrt{2}}\varphi(\frac{x}{2}), \varphi(x-k)> \\ &= \frac{1}{\sqrt{2}}\int_R \varphi(\frac{x}{2})\bar{\varphi}(x-k)dx. \end{aligned}$$

Eq. (4) is called *two-scale equation*. Using Fourier transforms on both sides of Eq. (4) produces the formula:

$$\hat{\varphi}(2\omega) = H(\omega)\hat{\varphi}(\omega), \tag{5}$$

where

$$H(\omega) = \frac{1}{\sqrt{2}}\sum_{k\in k} h_k e^{-ik\omega}.$$

Further analysis indicates that the sequence $\{h_k\}$ or its equivalent function $H(\omega)$ is very important. The multiresolution depends completely on it. $\{h_k\}$ is called *frequency response*, and $H(\omega)$ is called *transform function*.

Let us now recall the orthogonal decomposition of V_{j-1} as given in Eq. (1); namely,

$$V_{j-1} = W_j \oplus V_j.$$

In this decomposition expression, the orthonormal basis of V_j has been constructed with a scaling function, which is exactly the function system $\{\varphi_{j,k}^{(x)}, k \in \mathbb{Z}\}$. The problem that remains is how to construct the orthonormal basis for space W_j. In order to solve this problem, we first obtain a wavelet function $\psi(x)$ based on the scaling function $\varphi(x)$, and then derive the orthonormal basis of W_j from the wavelet function.

Definition 2.3 Let $g_k = (-1)^{k-1}\overline{h}_{1-k}$. $\psi(x)$ is defined as a wavelet function if the following condition is satisfied:

$$\frac{1}{\sqrt{2}}\psi(\frac{x}{2}) = \sum_{k\in\mathbb{Z}} g_k\varphi(x-k), \tag{6}$$

Eq. (6) implies that $\psi(\frac{x}{2}) \in V_0$. Further, based on Properties 3 and 4 of Definition 2.1, it is known that $\psi(x) \in V_1$. Now, if we apply Fourier transform, we obtain:

$$\begin{aligned} \hat{\psi}(2\omega) &= \sum_{k\in\mathbb{Z}} \frac{1}{\sqrt{2}} g_k e^{-ik\omega}\hat{\varphi}(\omega) \\ &= G(\Omega)\hat{\varphi}(\omega) \\ &= G(\Omega)\prod_{j=1}^{\infty} H(\frac{j\omega}{2}) \end{aligned} \tag{7}$$

where

$$G(\omega) = \sum_{k\in\mathbb{Z}} \frac{1}{\sqrt{2}} g_k e^{-ik\omega} \tag{8}$$

So far as the wavelet function $\psi(x)$ is concerned, we shall provide the following theorem, which along with Theorem 2.1, shall lay down the foundation for the orthogonal decomposition of V_{j-1}.

Theorem 2.2 Let $\psi_{j,k} = 2^{-1/2}\psi(2^{-j}x - k)$. Thus function system $\{\psi_{j,k}^{(x)}, k \in \mathbb{Z}\}$ forms the orthonormal basis of W_j.

From Theorem 2.2, it can be said that the orthonormal basis of W_j is obtained from wavelet function $\psi(x)$ by a binary dilation and a dyadic translation. The proof of Theorem 2.2 can be found in [1, 2].

Theorem 2.3 Let $H(\omega)$ be form of

$$H(\omega) = \left(e^{-i\omega/2}\cos\frac{\omega}{2}\right)^2 e^{-i\omega/2}\left(\cos\frac{\omega}{2} + i\sqrt{3}\sin\frac{\omega}{2}\right)$$

Then $H(\omega)$ satisfies the conditions listed in the following:

$$H(\omega) = \sum_{k\in\mathbb{Z}} \frac{1}{\sqrt{2}} h_k e^{-i\omega k} \in C([0, 2\pi])$$

$$H(0) = 1$$

$$\sum_{k\in\mathbb{Z}} |h_k||k|^{\epsilon} < \infty, \qquad 0 < \epsilon \leq 1$$

$$|H(\omega)|^2 + |H(\omega+\pi)|^2 = 1$$

$H(\omega)$ satisfies the Cohen condition

Consequently, equation

$$\hat{\varphi}(\omega) = \prod_{j=1}^{\infty} H(2^{-j}\omega) \in L^2(\mathbb{R}) \cap C([0, 2\pi])$$

is held, and $\{\varphi(x-k), k \in \mathbb{Z}\}$ constructs an orthonormal system.

3 Sub-patterns by Wavelet Decomposition

As can be realized, any real-world instruments for measuring physical data are capable of acquiring information with limited precision. In other words, the signals obtained using such instruments will have limited resolution. The same is also true for the one-dimensional pattern that we have derived in the preceding sections, $f(x)$; it must belong to

a closed space V_j. Mathematically, we can express this as follows:

$$A_j \ : \ L^2(I\!R) \Longrightarrow V_j$$
$$D_j \ : \ L^2(I\!R) \Longrightarrow W_j$$

Since $f(x) \in V_j \subset L^2(I\!R)$,

$$\begin{aligned} f(x) &= A_j f(x) = \sum_{k \in Z\!\!Z} c_{j,k} \varphi_{j,k}(x) \\ &= \sum_{m \in Z\!\!Z} c_{j+1,m} \varphi_{j+1,m}(x) \\ &+ \sum_{m \in Z\!\!Z} d_{j+1,m} \psi_{j+1,m}(x) \end{aligned} \tag{9}$$

where

$$c_{j+1,m} =< A_{j+1} f, \varphi_{j+1,m} >= \sum_{k \in Z\!\!Z} c_{j,k} \hat{h}_{k-2m} \tag{10}$$

$$d_{j+1,m} =< D_{j+1} f, \psi_{j+1,m} >= \sum_{k \in Z\!\!Z} c_{j,k} \hat{g}_{k-2m} \tag{11}$$

and $\hat{h}_{k-2m}$ and $\hat{g}_{k-2m}$ denote the conjugate vectors of h_{k-2m} and g_{k-2m}, respectively. When both h_{k-2m} and g_{k-2m} are real, we have $\hat{h}_{k-2m} = h_{k-2m}$ and $\hat{g}_{k-2m} = g_{k-2m}$.

It should be mentioned that both Eqs. (10) and (11) compute the sum of an infinite number of terms. However, from a computational point of view, we wish to see only a finite number of non-zero terms, h_k, hence reducing the problem of infinite summation to that of finite summation. In doing so, we carry out the following procedure, in order to find the expression

$$H(\omega) = \sum_{k \in Z\!\!Z} \frac{1}{\sqrt{2}} h_k e^{-ik\omega},$$

such that the number of non-zero h_k is finite.

First, let us consider:

$$1 = \left(\cos^2 \frac{\omega}{2} + \sin^2 \frac{\omega}{2}\right)^3. \tag{12}$$

Suppose that

$$| H(\omega) |^2 = \cos^6 \frac{\omega}{2} + 3 \cos^4 \frac{\omega}{2} \sin^2 \frac{\omega}{2}, \tag{13}$$

hence,

$$| H(\omega + \pi) |^2 = \sin^6 \frac{\omega}{2} + 3 \sin^4 \frac{\omega}{2} \cos^2 \frac{\omega}{2}. \tag{14}$$

Since,

$$\frac{1 + e^{-i\omega/2}}{2} = \frac{e^{-i\omega/2}(e^{i\omega/2} + e^{-i\omega/2})}{2} = e^{-i\omega/2} \cos \frac{\omega}{2} \tag{15}$$

$$\frac{1 - e^{-i\omega/2}}{2} = \frac{e^{-i\omega/2}(e^{i\omega/2} - e^{-i\omega/2})}{2} = i e^{-i\omega/2} \sin \frac{\omega}{2} \tag{16}$$

we have:

$$H(\omega) = (e^{-i\omega/2} \cos \frac{\omega}{2})^2 e^{-i\omega/2} (\cos \frac{\omega}{2} + i\sqrt{3} \sin \frac{\omega}{2}) \tag{17}$$

at the same time, we know:

$$H(\omega) = \sum_{k=0}^{3} \frac{1}{\sqrt{2}} h_k e^{-ik\omega} \tag{18}$$

By comparing Eqs. (17) and (18), we can immediately obtain the following:

$$\begin{aligned} h_0 &= \frac{1 + \sqrt{3}}{4\sqrt{2}} = 0.4829629131445341 \\ h_1 &= \frac{3 + \sqrt{3}}{4\sqrt{2}} = 0.8365163037378077 \\ h_2 &= \frac{3 - \sqrt{3}}{4\sqrt{2}} = 0.2241438680420134 \\ h_3 &= \frac{1 - \sqrt{3}}{4\sqrt{2}} = -0.1294095225512603 \end{aligned}$$

Thus, we can simplify the wavelet transform expressions of Eqs. (10) and (11) into the following:

$$c_{j+1,m} = \sum_{k=0}^{3} h_k c_{j,k+2m} \tag{19}$$

$$d_{j+1,m} = \sum_{k=0}^{3} g_k c_{j,k+2m} \tag{20}$$

Next, $H(\omega)$ is also determined following the above mentioned steps, except that we examine the expression of

$$1 = \left(\cos^2 \frac{\omega}{2} + \sin^2 \frac{\omega}{2}\right)^5$$

to obtain

$$H(\omega) = \sum_{k=0}^{5} \frac{1}{\sqrt{2}} h_k e^{-ik\omega}.$$

In this case, we can simplify the wavelet transform expressions of Eqs. (10) and (11) into the following:

$$c_{j+1,m} = \sum_{k=0}^{5} h_k c_{j,k+2m} \tag{21}$$

$$d_{j+1,m} = \sum_{k=0}^{5} g_k c_{j,k+2m} \tag{22}$$

In *Ten Lectures on Wavelets* [2], I. Daubechies used the following notations:

$$nM_0(\xi) = \frac{1}{\sqrt{2}} \sum_{n=0}^{2N-1} Nh_n e^{-in\xi} \qquad (23)$$

where $nM_0(\xi)$ is equivalent to $H(\omega)$ in our case, and Nh_n is equivalent to our h_k.

In [2], Daubechies also provided the exact values of h_k (or Nh_n) for $N = 2$ to 10 in tabular forms. (The tables might be of interest to those readers who want to use Eqs. (10) and (11) but not to know how h_k's are computed.) When N is large enough, the computation of h_k could become problem-dependent. Generally speaking, the larger the N value, the higher the resolution of the wavelet orthonormal decomposition will be, and at the same time, the more costly the computation will become.

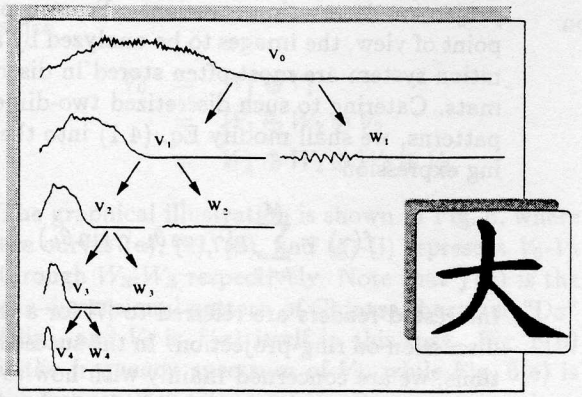

Figure 1: Examples of the wavelet transform sub-patterns from a Chinese character

In Fig. 1, we have shown the one-dimensional pattern resulted from the ring-projection [7] of a two-dimensional pattern, for example, a Chinese character, and its corresponding wavelet transform sub-patterns. In the figure, V_0 denotes the resulting one-dimensional pattern. V_j denotes the wavelet transform sub-pattern resulted from the jth wavelet transform based on Eq. (21). W_j denotes the wavelet transform sub-pattern resulted from the jth wavelet transform based on Eq. (22). Since

$$\begin{aligned} V_j &= W_{j+1} \oplus V_{j+1} \\ &= W_{j+1} \oplus W_{j+2} \oplus V_{j+2} \\ &= W_{j+1} \oplus W_{j+2} \oplus W_{j+3} \oplus V_{j+3} \\ &= \cdots\cdots\cdots. \end{aligned}$$

It can be seen that in Fig. 1,

$$\begin{aligned} V_0 &= W_1 \oplus V_1 \\ &= W_1 \oplus W_2 \oplus V_2 \\ &= W_1 \oplus W_2 \oplus W_3 \oplus V_3 \\ &= W_1 \oplus W_2 \oplus W_3 \oplus W_4 \oplus V_4. \end{aligned}$$

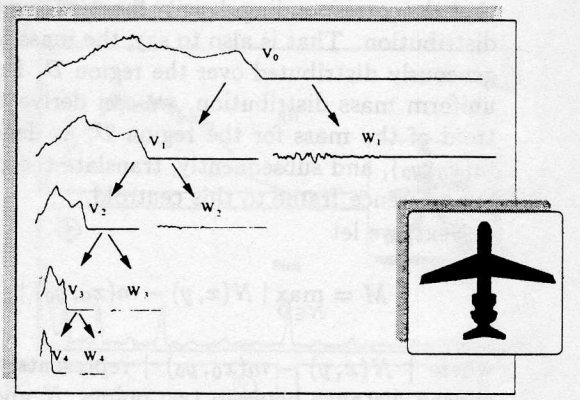

Figure 2: Examples of the wavelet transform sub-patterns from a pattern

Some examples of the wavelet transform sub-patterns from a pattern are shown in Fig. 2

4 Experiments

It is a well-known fact that in many real-life pattern recognition situations, patterns are often found to be rotated due to experimentation constraints or errors. This implies that the new pattern recognition method must be developed that is invariant to rotations. In 1991, Tang [7] first proposed a method of transforming two-dimensional patterns into one-dimensional patterns through so-called *ring projections*. As the projections are done in the form of rings, the one-dimensional pattern obtained from ring-projection is invariant to rotations.

4.1 Dimension Reduction of Two-Dimensional Patterns

This section provides an overview of the ring-projection method for reducing the dimensionality of two-dimensional patterns. First, suppose that a two-dimensional pattern such as a Chinese character has been represented by a binary image. Taking a Chinese character "big" as an example, its grey-scale image, $p(x, y)$, can be discretized into binary values as follows:

$$p(x,y) = \begin{cases} 1 & \text{if } (x,y) \in \mathcal{D} \\ 0 & \text{otherwise} \end{cases} \qquad (24)$$

where domain $\mathcal{D}$ corresponds to the white region of the character, as shown in Fig. 3. The above multivariate function $p(x, y)$ can also be viewed as a two-dimensional density function of mass distribution on the plane. From Eq. (24), it is readily noted that the corresponding density function is a uniform distribution. That is also to say, the mass is homogeneously distributed over the region $\mathcal{D}$. From this uniform mass distribution, we can derive the centroid of the mass for the region $\mathcal{D}$, as denoted by $m(x_0, y_0)$, and subsequently, translate the origin of our reference frame to this centroid.

Next, we let

$$M = \max_{N \in \mathcal{D}} \mid N(x, y) - m(x_0, y_0) \mid$$

where $\mid N(x, y) - m(x_0, y_0) \mid$ represents the Euclidean distance between two points, N and m, on the plane. Further, we transform the original reference Cartesian frame into a polar frame based on the following relations:

$$\begin{cases} x &= \gamma \cos\theta \\ y &= \gamma \sin\theta \end{cases}$$

Hence,

$$p(x, y) = p(\gamma \cos\theta, \gamma \sin\theta)$$

where $\gamma \in [0, \infty)$, $\theta \in (0, 2\pi]$.

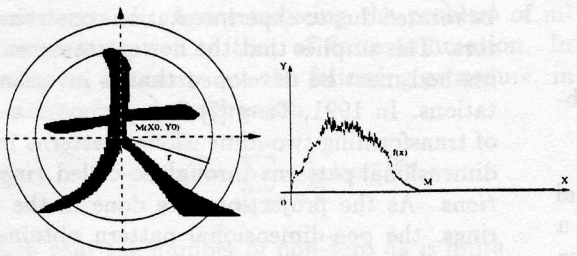

Figure 3: An example of dimension reduction for Chinese character "big"

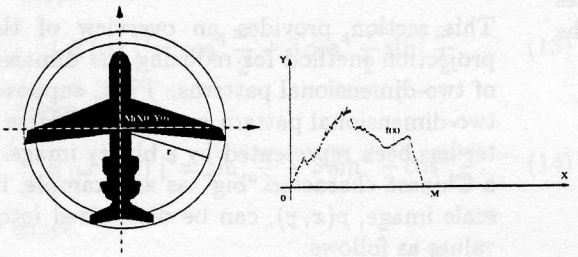

Figure 4: An example of dimension reduction for a two-dimensional pattern

For any fixed $\gamma \in [0, M]$, we then compute the following integral:

$$f(\gamma) = \int_0^{2\pi} p(\gamma \cos\theta, \gamma \sin\theta) d\theta$$

The resulting $f(\gamma)$ is in fact equal to the total mass as distributed along circular rings. Hence, the derivation of $f(\gamma)$ is also termed as a ring-projection of the planar mass distribution. The single-variate function $f(\gamma)$, $\gamma \in [0, M]$, sometimes also denoted as $f(x)$, $x \in [0, M]$, can be viewed as a one-dimensional pattern that is directly transformed from the original two-dimensional pattern through a ring-projection. Owing to the facts that the centroid of the mass distribution is invariant to rotation and that the projection is done along circular rings, the derived one-dimensional pattern will be invariant to the rotations of its original two-dimensional pattern. In other words, the ring-projection is rotation-invariant. From a practical point of view, the images to be analyzed by a recognition system are most often stored in discrete formats. Catering to such discretized two-dimensional patterns, we shall modify Eq. (4.1) into the following expression

$$f(\gamma) = \sum_{k=0}^{M} p(\gamma \cos\theta_k, \gamma \sin\theta_k) \qquad (25)$$

Interested readers are referred to [7] for a thorough discussion on ring-projection. In the succeeding sections, we are concerned mainly with how to extract as much information as possible from the obtained ring-projection, i.e., an one-dimensional pattern, by way of wavelet transform. This, as will be described later, enables us to obtain a set of wavelet transform sub-patterns – curves that are non-self-intersecting, from which feature vectors defined over the curves' fractal dimensions can be computed easily.

Another example of dimension reduction for a two-dimensional pattern can be found in Fiog. 4.

4.2 Results

This section presents the procedure as well as the results of our experiments that aim at recognizing a set of two-dimensional patterns, including a sub-set of Chinese characters plus 52 upper and lower case English letters. All samples were rotated at different angles. Examples of Chinese character "Xin" (in English it means heart) and English letter "g" rotated at 0°, 75°, 150°, 225°, and 300° are illustrated in Fig. 5.

In our experiments, we performed three consecutive wavelet transform for each one-dimensional

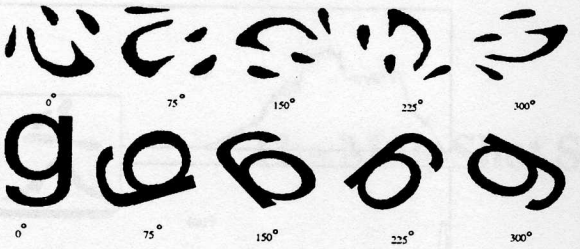

Figure 5: Examples of Chinese character "Xin" (Heart) and English letter "g" rotated at 0°, 75°, 150°, 225°, and 300°.

pattern. Hence, the one-dimensional pattern, such as the ring-projection of Chinese character "Da" (in English it means big), will yield seven non-self-intersecting curves, namely,

$$V_0,\ V_1,\ V_2,\ V_3,\ W_1,\ W_2,\ W_3,$$

since

$$\begin{aligned} V_0 &= W_1 \oplus V_1 \\ &= W_1 \oplus W_2 \oplus V_2 \\ &= W_1 \oplus W_2 \oplus W_3 \oplus V_3. \end{aligned}$$

The graphical illustration is shown in Fig. 6, where the curves (a), (c), (d), and (g)-(j) represent V_0-V_3 through W_3-W_3 respectively. Note that $f(x)$ is the one-dimensional pattern of Chinese character "Da" (Big), and V_0 is $f(x)$ itself in this case. Fig. 6(b) is the frequency spectrum of V_0, while Fig. 6(e) is the frequency spectrum of V_1. By comparing these two frequency spectra, we can find that V_0 contains all frequency components of $f(x)$, while V_1 contains only one half of frequency components of $f(x)$. The reason is that V_0 is divided into two parts:

$$V_0 = V_1 \oplus W_1,$$

As for the first part, V_1, only the low-frequency components of V_0 are kept, and the high-frequency components are lost. In addition, only the high-frequency components of V_0 are kept, and the low-frequency components are lost in W_1. Similarly, V_1 is further divided into two parts:

$$V_1 = V_2 \oplus W_2,$$

where, the low-frequency components of V_1 remain in V_2, while the high-frequency components of V_1 are kept in W_2. Hence, V_2 contains only one half of frequency components of V_1, that is only one quarter of frequency components of $f(x)$. Again for the same reason, V_3 contains only one eighth of frequency components of $f(x)$, etc..

For each of the seven curves, we further computed its divider dimension [3], and therefore, related each character with a feature vector.

A series of experiments have been conducted to verify the proposed method. The results are shown in Figs. 6 - 8.

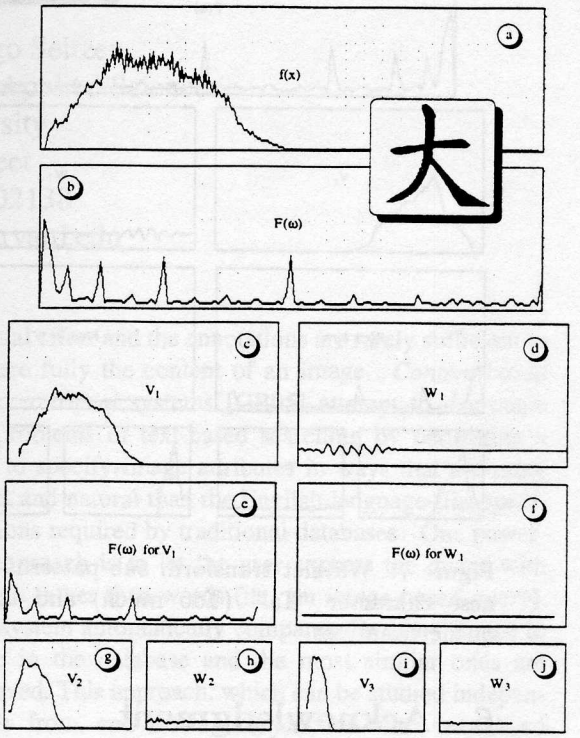

Figure 6: Wavelet transform sub-patterns of Chinese character "Da" (Big) and their frequency analyses.

5 Conclusion

In this paper, we described an efficient approach to optical character recognition including Chinese character recognition that utilizes a novel formulation of feature vectors. Prior to the computation of feature vectors, we employed a ring-projection method to reduce the dimensionality of the original input pattern, and a wavelet transform technique to transform the derived pattern into a set of sub-patterns, from which the feature vectors can readily be computed. Experimental validations on the validity of the presented scheme for the feature construction and recognition of characters were also mentioned, in the paper, with illustrations. One of the interesting extensions from the present work would be to compare the empirical results of our approach with those of existing approaches.

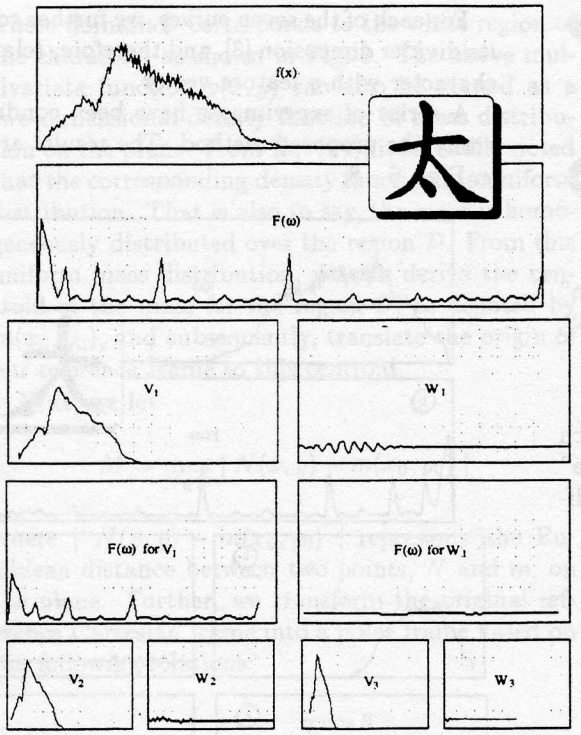

Figure 7: Wavelet transform sub-patterns of Chinese character "Tai" (Too much) and their frequency analyses.

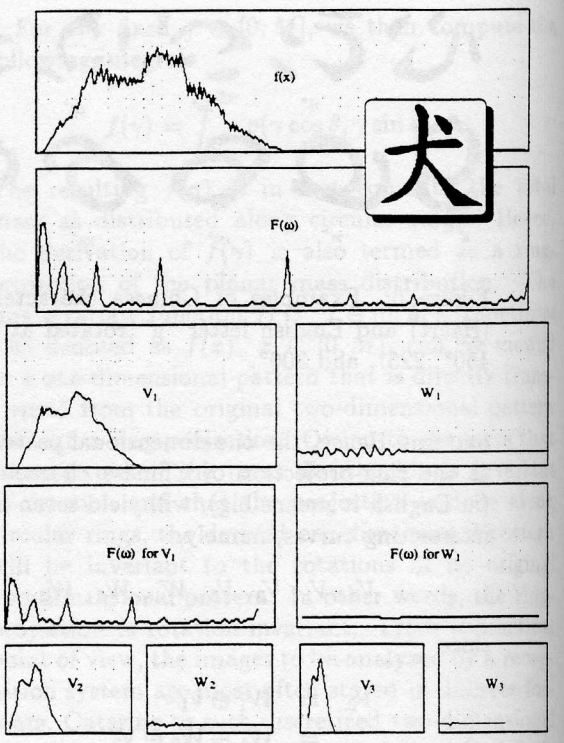

Figure 8: Wavelet transform sub-patterns of Chinese character "Quan" (Dog) and their frequency analyses.

6 Acknowledgment

This work was supported by research grants received from Research Grant Council (RGC) of Hong Kong, and Faculty Research Grant (FRG) of Hong Kong Baptist University. This work was also supported by the Ministry of Education of the People's Republic of China, and Sichuan University, China. We wish to express our gratitude to the staff members at the Sichuan University, China, for their assistance to this research project.

References

[1] C. K. Chui. *An Introduction to Wavelets,* Boston: Academic Press, 1992.

[2] I. Daubechies. "Ten Lectures on Wavelets," *CBMS - Conference Lecture Notes,* Vol. 61, SIAM Philadelphia, 1991.

[3] K. L. Falconer. *Fractal Geometry: Mathematical Foundation and Applications,* New York: Wiley, 1990.

[4] S. Mallat. "A theory of multiresolution signal decomposition: the wavelet representation," *IEEE Trans. on Pattern Analysis and Machine Intelligence,* Vol. 11, pp. 674-693, 1989.

[5] S. Mallat. "Multiresolution approximations and wavelet orthonormal bases of $L^2(R)$," *Trans. Amer. Math. Soc.* Vol. 315, pp. 69-87, 1989.

[6] S. Mallat. Multiresolution representation and wavelets, *Ph. D. Thesis,* University of Pennsylvania, Philadelphia, PA, 1988.

[7] Y. Y. Tang, H. D. Cheng, and C. Y. Suen. "Transformation - ring - projection (TRP) algorithm and its VLSI implementation," *Int. Journal of Pattern Recognition and Artificial Intelligence,* Vol. 5, No. 1-2, pp. 25-56, 1991.

[8] Y. Y. Tang, Hong Ma, Dihua Xi, Yi Cheng, and C. Y. Suen. "Extraction of reference lines from document with grey-level background using sub-image of wavelets," *Proc. 3-nd Int. Conf. on Document Analysis and Recognition,* Montreal, Canada, Oct. 14-16, 1995, pp. 571-574.